Journal of Asian Earth Sciences 69 (2013) 48–59

Contents lists available at SciVerse ScienceDirect

Journal of Asian Earth Sciences

journal homepage: www.elsevier.com/locate/jseaes

Major changes in East Asian climate in the mid-Pliocene: Triggered by the uplift of the Tibetan Plateau or global cooling?

Junyi Ge [a,b,*], Ying Dai [a,c], Zhongshi Zhang [d,e,f], Deai Zhao [a], Qin Li [a], Yan Zhang [a], Liang Yi [g], Haibin Wu [a], Frank Oldfield [h], Zhengtang Guo [a]

[a] Key Laboratory of Cenozoic Geology and Environment, Institute of Geology and Geophysics, Chinese Academy of Sciences, Beijing 100029, China
[b] The Laboratory of Human Evolution, Institute of Vertebrate Palaeontology and Palaeoanthropology, Chinese Academy of Sciences, Beijing 100044, China
[c] Institute of Tibetan Plateau Research, Chinese Academy of Sciences, Beijing 100101, China
[d] Bjerknes Centre for Climate Research, Allegaten 55, 5007 Bergen, Norway
[e] UNI Research, Allegaten 55, 5007 Bergen, Norway
[f] Nansen-Zhu International Research Center, Institute of Atmospheric Physics, Chinese Academy of Sciences, Beijing 100029, China
[g] State Key Laboratory of Lithospheric Evolution, Institute of Geology and Geophysics, Chinese Academy of Sciences, Beijing 100029, China
[h] School of Environmental Sciences, University of Liverpool, Liverpool L69 7ZT, UK

ARTICLE INFO

Article history:
Available online 17 October 2012

Keywords:
Mid-Pliocene
East Asian monsoon
Tibetan Plateau
Global cooling

ABSTRACT

Since the mid-Pliocene, East Asian climates have experienced significant changes. One view suggests that significant uplift of the Tibetan Plateau during this period could have been responsible for these dramatic changes in the strength of the East Asian monsoon and for Asian interior aridification, while some other authors attribute these changes to the ongoing global cooling and rapid growth of the Arctic ice-sheet. Up to the present, which factor dominates the major changes of East Asian climate in the mid-Pliocene is still a contentious issue. This study presents an analysis of several climate proxies including grain-size, $(CaO^* + Na_2O + MgO)/TiO_2$ ratio, Na/Ka ratio and dust accumulation rates of the Xifeng Red Clay sequence in the eastern Chinese Loess Plateau and the Xihe Pliocene loess-soil sequence in West Qinling. They reveal that aridity in the continental interior and winter monsoon circulation both intensified, whereas the East Asian summer monsoon showed a weakening rather than intensifying trend since the mid-Pliocene. These changes are also supported by the other multi-proxy records from various regions in East Asia. Previous numerical modeling studies have demonstrated that uplift of the Tibetan Plateau would have simultaneously enhanced continental-scale summer and winter monsoon strength as well as central Asian aridity. The mid-Pliocene climate changes in East Asia are therefore unlikely to be a response to Plateau uplift. On the contrary, our recent modeling results give support to the view that ongoing cooling could have intensified both the aridity of the interior and the strength of the winter monsoon, but weakened the summer monsoon in East Asia.

1. Introduction

The mid-Pliocene was a critical period, during which both the East Asian and global climates experienced major changes. In this period, the Earth's climate underwent a significant cooling with rapid expansion of the Northern Hemisphere ice-sheets (Shackleton et al., 1995), and a significant intensification of Asian interior aridity (Rea et al., 1998; An et al., 2001; Guo et al., 2004). At the same time, in the Chinese Loess Plateau (CLP), the grain-size of eolian deposits coarsened remarkably, suggesting continuous strengthening of the East Asian monsoon circulation at ~3.6 Ma ago (An et al., 2001). Meanwhile, the mid-Pliocene was also considered to be a period with strong tectonic activity over the Tibetan Plateau (TP). Enhanced TP uplift after ~3.6 Ma was inferred from the rapid accumulation of widely distributed conglomerates and the sharp increase in sediment fluxes in many basins along the northeastern and eastern margins of the TP (Li and Fang, 1999; Zheng et al., 2000; Fang et al., 2005), from the strengthened activities of some faults in the northeastern margin of TP (Yuan, 2003; Hough et al., 2011), and from rapid exhumation on the Plateau (Wang et al., 2011).

On the basis of abundant observational evidence of the tectonic movements, some authors have suggested that significant uplift of the TP occurred in the mid-Pliocene and led to dramatic changes in the strength of the East Asian monsoon and in Asian interior aridification (e.g., Li and Fang, 1999; An et al., 2001). Others have argued that the conglomerate deposits and the increased

* Corresponding author at: Key Laboratory of Cenozoic Geology and Environment, Institute of Geology and Geophysics, Chinese Academy of Sciences, Beijing 100029, China. Tel.: +86 10 82998382; fax: +86 10 62032495.
E-mail address: gejunyi@gmail.com (J. Ge).

1367-9120/$ - see front matter © 2012 Elsevier Ltd. All rights reserved.
http://dx.doi.org/10.1016/j.jseaes.2012.10.009

sedimentation rates were both possibly caused by climatic changes rather than tectonic uplift (Zhang et al., 2001; Molnar, 2004; Heermance et al., 2007), and that the strengthened interior aridity and winter monsoon intensity could be attributed to the rapid growth of the Arctic ice-sheet (Guo, 2003; Lu et al., 2010). Whether these changes in the East Asian environment were mainly induced by tectonic uplift or by climatic changes, and the extent to which the TP uplift influenced the Asian climates during the Mid-Pliocene, are still issues in debate.

Over the past decades, a number of numerical modeling experiments have been performed to investigate the climatic effects of Cenozoic TP uplift. It was found that TP uplift can give rise simultaneously to several linked climatic consequences, i.e., intensification of both the East Asian winter monsoon (EAWM) circulation and East Asian summer monsoon (EASM) precipitation, as well as increased aridity of the continental interior (e.g., Kutzbach et al., 1989; Broccoli and Manabe, 1992; An et al., 2001; Liu and Yin, 2002; Abe et al., 2003). Thus, reconstructing the history of the East Asian monsoon and interior aridity using geological records, and comparing the results with numerical model simulations may provide critical information regarding TP uplift and the mechanism responsible for East Asian climate changes during the mid-Pliocene.

The widespread eolian deposits on the Eurasian continent, covering a time from the early Miocene to the Holocene, are considered to be some of the most detailed and long-term records of late Cenozoic climate change (Liu, 1985; Markovic et al., 2011; Guo et al., 2002), and are of particular value for providing insight into the history of continental interior aridification. They also record changes in regional atmospheric systems (Markovic et al.,

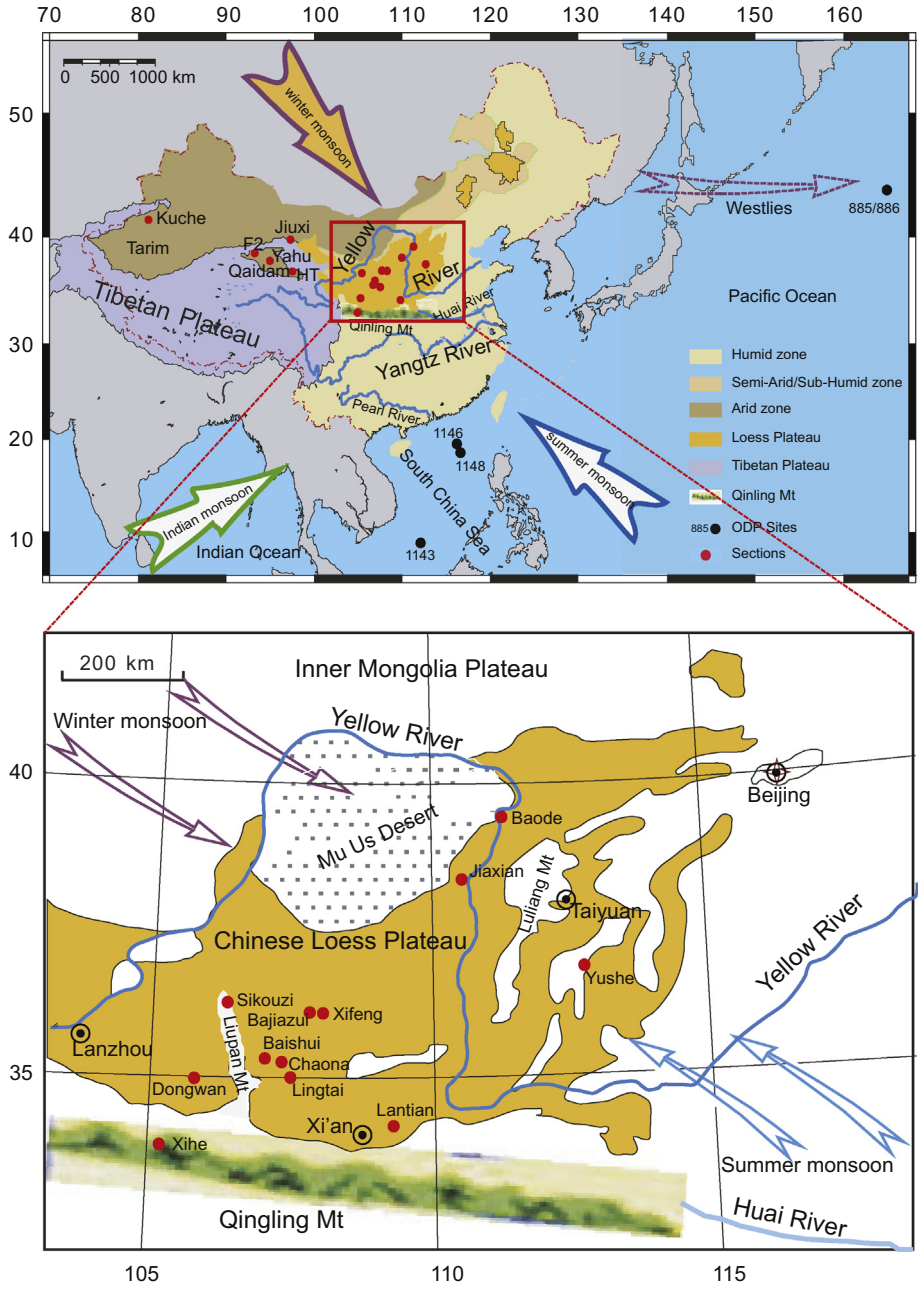

Fig. 1. Map showing the location of the multi-proxy records in the Northwest Arid areas including the Baikal, Qaidam, Tarim and Jiuxi Basins, in the Chinese Loess Plateau, in the Pacific Ocean and in the South China Sea.

2008, 2009; Buggle et al., 2011), such as the evolution of the East Asian monsoon (Ding et al., 1999; An et al., 2001; Guo et al., 2002, 2008). In the past decades, much knowledge of past environmental changes in the mid-Pliocene has been derived from the Red Clay sequences in the eastern CLP. Nevertheless, further studies are necessary since some palaeoenvironmental proxies are poorly understood and open to alternative interpretations (Sun et al., 1998; Jiang et al., 2008; Suarez et al., 2011). As a consequence, the evolution of the East Asian climate, especially of the summer monsoon in the mid-Pliocene, remains open to alternative explanations (Wu et al., 2006; Clemens et al., 2008; Suarez et al., 2011). In recent years, several loess-soil sequences spanning 22.0–3.5 Ma have been found in the western CLP (e.g., Guo et al., 2002, 2008; Hao and Guo, 2004, 2007; Liu et al., 2005; Zhan et al., 2010) and West Qinling (Ge and Guo, 2010). These sequences contain several features that distinguish them from the Red Clay in the eastern CLP (Hao and Guo, 2004), for example, much clearer loess-soil alternations and fewer indications of syn- and post-depositional modification (Hao and Guo, 2004).

In this paper, grain-size, dust accumulation rates and chemical weathering were compared between the contemporary eolian deposits in the eastern CLP and those in West Qinling in order to clarify the climatic implications of these proxies. We then compare these results with multi-proxy records from various regions in East Asia (Fig. 1) to reconstruct more securely changes in the East Asian monsoon and interior aridity. By comparing the empirically derived geological evidence with numerical modeling results, we attempt to provide insight into the effects of TP uplift and the mechanisms driving East Asian climate change during the mid-Pliocene.

2. Material and methods

The Xifeng section (107°58′E, 35°53′N, ~1300 m a.s.l.) is one of the typical Pliocene Red Clay sequences in the central part of the eastern CLP (Fig. 1). This section lies on a substrate of lacustrine sediments and is overlain by the Quaternary loess-soil sequence spanning the past 2.6 Ma. It has a thickness of 55.9 m with a basal age of ~7.6 Ma (Sun et al., 1998). The mean annual temperature of this region varies from 8.9 to 9.1 °C, and the mean annual precipitation ranges from 580 to 590 mm. Previous studies have shown that the lower section, older than 6.2 Ma, is a water-reworked deposit (Guo et al., 2001), while the upper part of this section is of eolian origin. In the present study, only the upper 48 m (~6.0–2.6 Ma) of the Red Clay sequence was investigated and 480 bulk samples at 10 cm interval were collected.

The Xihe loess-soil sequence (34°04′N, 105°23′E) was also sampled for comparison. The Xihe section is located in the alluvial highlands surrounding the Xihe basin (Fig. 1), and exposed along the flanks of an elongated gully with a top elevation of 1875 m a.s.l. It is 150.2 m thick and was paleomagnetically dated to a period from 10.4 Ma to 4.1 Ma (Ge and Guo, 2010; Ge et al., 2012). The mean annual temperature and precipitation at Xihe are ~8.4 °C and ~555 mm, respectively. 460 bulk samples were collected at 10 cm interval from the upper 46 m (6.0–4.1 Ma).

The detailed ages were obtained by interpolation of magnetic susceptibility sequences from Xifeng (Fig. 2a) (Guo et al., 2001) and Xihe (Fig. 2b) (Ge et al., 2012) using the Kukla et al. (1988) method and age controls from the magnetostratigraphic results (Sun et al., 1998; Ge et al., 2012), and then eolian dust accumulation rates were calculated. The grain-size at 0.2–0.5 m intervals from Xihe sequence was analyzed using the protocols and equipment described in Qiao et al. (2006).

In this study, the chemical composition of 180 bulk samples at 0.2–0.5 m intervals for the Xihe section was also analyzed. Organic carbon and carbonate were removed successively from the bulk samples by using 1 M acetic acid and 30% H_2O_2 respectively. 0.7 g powdered subsamples mixed with 7.0000 g $Li_2B_4O_7$ were heated to 1100 °C in a Pt crucible then cooled as a glass disc for chemical composition measurements. Major element abundances were determined using a Panalytical AXIOS XRF spectrometer in the Institute of Geology and Geophysics, Chinese Academy of Sciences. All major element percentages were converted to oxide percentages. Analytical uncertainties are ±2% for all major elements except P_2O_5 and MnO (up to ±5%).

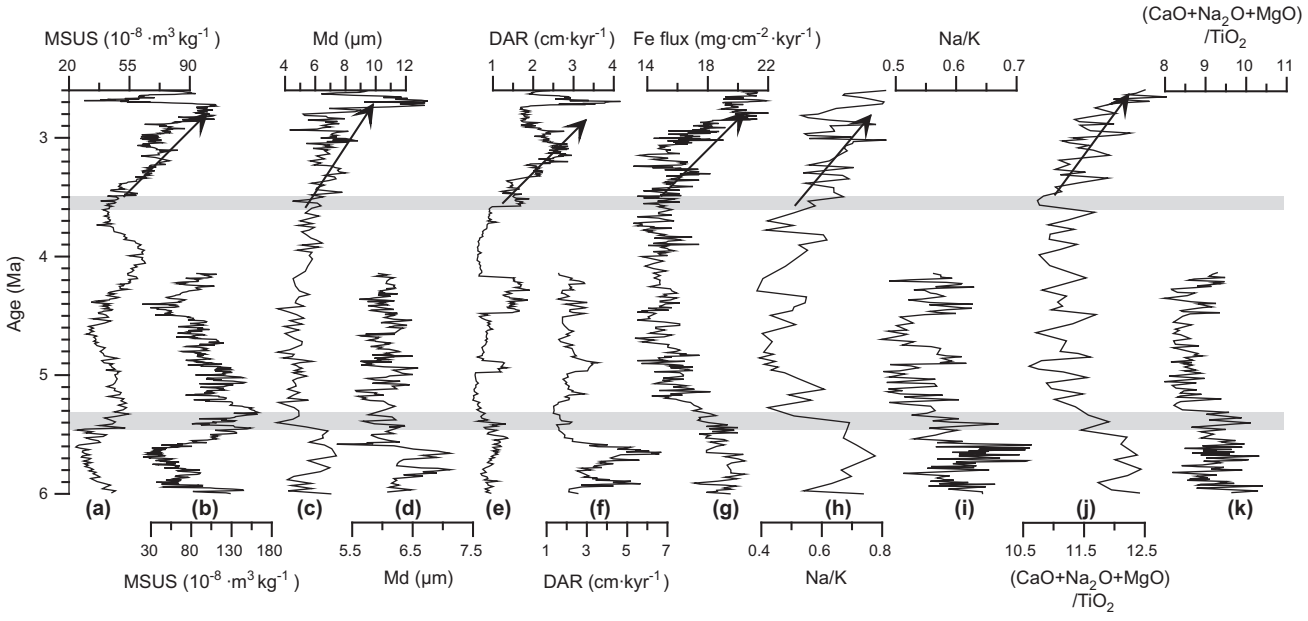

Fig. 2. Variations in magnetic susceptibility, grain-size, dust accumulation rate, Fe flux and chemical weathering ratio in the Xifeng Red Clay section and the Xihe Pliocene loess-soil section. Data for magnetic susceptibility of Xihe and Xifeng are from Ge et al. (2012) and Guo et al. (2001), and data for grain-size of Xifeng sequence is from Guo et al. (2004).

3. Results

3.1. Magnetic susceptibility

Magnetic susceptibility (MS) is usually used as an important tool for stratigraphic correlation of the Miocene–Quaternary eolian deposits in CLP (Kukla and An, 1989; Hao and Guo, 2007). There is a general similarity between the MS sequences for both Xifeng and Xihe sections after ~6 Ma (Fig. 2a and b), attesting to the relative continuity of eolian accumulation on the CLP.

3.2. Grain size

The grain-size sequence for Xihe late Miocene–Pliocene loess-soil sections demonstrate similar variations with that for the Xifeng Red Clay (Guo et al., 2004), but with slightly coarser textures over the same time period (Fig. 2c and d). The median grain-size at Xihe is ~1 μm coarser on average than at Xifeng (Fig. 2c and d). The similarity of time-dependent variations and the spatial pattern, coarser in the western Loess Plateau and finer in the eastern Plateau (Liu, 1985), are also consistent with similar features in the Quaternary loess, providing further confirmation that the grain-size variations for the two sections can be used for EAWM reconstruction.

The grain-size sequences for both Xifeng and Xihe sections can be visually divided into three periods. Prior to ~5.4 Ma, the median grain size (Md) of the two sections varies from 6.0 to 7.1 μm and from 4.2 to 7.4 μm, respectively. For the period ~5.4–3.6 Ma, grain size is ~1 μm finer than that before ~5.4 Ma with low fluctuations. After ~3.6 Ma, the grain-size in the Xifeng section begins to coarsen gradually from 5.2 to 13.3 μm (average 9.2 μm) and the amplitude of the fluctuations also increases markedly from ~3.6 to 2.6 Ma, indicating significant intensification of the EAWM.

3.3. Dust accumulation rates and depositional fluxes

Dust accumulation rates and depositional fluxes for eolian deposits, expressed by Al-flux or Fe-flux, have often been used to evaluate the aridity of the continental interior (An et al., 2001; Liu and Ding, 1998). Variations in the dust accumulation rate at Xihe (Fig. 2f) are essentially consistent with those at Xifeng (Fig. 2e), as are the Fe-fluxes variations (Fig. 2g). The sequence of dust accumulation rates and Fe-fluxes at Xihe and Xifeng can be divided into three broad periods. From 6.0 to 5.4 Ma, it is characterized by relatively higher DAR and Fe-fluxes, especially in the Xihe section, indicating higher aridity in the source areas (Hovan et al., 1989) during this period. From 5.4 to 3.6 Ma, both DAR and Fe-fluxes in the two sections decreased, but with two short-lived peaks between 5.0 and 4.2 Ma recognizable in the DAR sequences. Since ~3.6 Ma, the dust accumulation rates and Fe-fluxes at Xifeng increased significantly, indicating intensified interior aridity in central Asian.

3.4. Chemical weathering intensity

The Na/K ratio (Nesbitt et al., 1980; Chen et al., 2001) (in molar proportions) and $(CaO^* + Na_2O + MgO)/TiO_2$ ratio (in molar proportions, $CaO*$ is the amount of CaO in silicates), are used to detect variations in chemical weathering for the Xifeng and Xihe sequences. The $(CaO^* + Na_2O + MgO)/TiO_2$ ratio has been shown to be a reliable proxy, independent of grain size, for the chemical weathering of loess (Yang et al., 2006). Some previous studies have also suggested that there are no significant changes in the provenance of the eolian deposits on CLP during the period 7–2.6 Ma (Sun, 2005; Wang et al., 2007; Sun and Zhu, 2010). Changes in the chemical composition of samples from the Xifeng and Xihe sequences can therefore provide information on variations in chemical weathering at the two sites studied here.

Variations in the $(CaO^* + Na_2O + MgO)/TiO_2$ ratio and Na/K ratio both show good correlation between the Xifeng Red Clay sequence (Fig. 2h, j) and the Xihe loess-soil sequence, but with larger fluctuations at Xihe (Fig. 2i and k). The $(CaO^* + Na_2O + MgO)/TiO_2$ and Na/K ratio curves for Xifeng and Xihe can be broadly divided at ~5.4 Ma and ~3.6 Ma, similar to the variations in the other proxies. Before ~5.4 Ma, the two sequences were both characterized by high $(CaO^* + Na_2O + MgO)/TiO_2$ and Na/K ratios, suggesting weak chemical weathering of the eolian deposits. From 5.4 to 3.6 Ma, chemical weathering intensity for both sequences increased, as shown by significantly decreasing of the two ratios. Since ~3.6 Ma, they increase abruptly from 10.7 to 12.9 and from 0.51 to 0.81 at Xifeng respectively, reflecting significant decreases in chemical weathering intensity at Xifeng after ~3.6 Ma.

4. Discussion

4.1. Extensive aridification of interior drylands in central Asia around 3.6 Ma

Thick eolian dust deposits, covering a time from the early Miocene to Holocene, spread widely across the middle reaches of the Yellow River in the CLP (Liu, 1985; Guo et al., 2010). A large collection of evidence indicates that most of these wind-blown silt deposits are mainly derived from extensive dryland areas in the interior of central Asia (Guo et al., 2008; Lu et al., 2010). Dry climates usually lead to an extension of the interior arid region, strengthened physical weathering and increased wind erosion, giving rise to more dust/silt for transport and deposition in downwind locations (Liu and Ding, 1998). This causes an increase in the dust flux and an increase in eolian dust cover in the downwind area (Kukla and An, 1989; Lu et al., 2010).

The dust accumulation rate of eolian dust and the Fe-flux at Xifeng (Fig. 3a and b) both significantly increased at ~3.6 Ma ago, indicating intensification of aridity in central Asia. The evidence for this aridification event corresponds with that from previous studies of other typical Red Clay sequences in the eastern CLP, such as Bajiazui (Fig. 3c) (An et al., 2001), Chaona (Fig. 3d) (Song et al., 2000), Lingtai (Fig. 3e) (Ding et al., 1998) and Jiaxian (Fig. 3f) (Qiang et al., 2001). By qualitatively reconstructing the distribution of the eolian deposits from early Miocene to Holocene, Lu et al. (2010) further showed that the eolian dust cover became more extensive from~3.6 Ma onwards. These records are broadly coincident with the sharp increase in eolian dust accumulation rate in the North Pacific (Fig. 3g) (Rea et al., 1998). All these evidence points to a major shift towards increased aridity in the central Asian interior around this time.

A number of studies have demonstrate that extensive drylands including the Gobi and deserts in Mongolia and northwest China, for example the Taklimakan, Qaidam, Tarim and some inland basins along the northeastern margin of the TP, are important source areas for eolian dust transported to the CLP and the North Pacific (e.g., Liu, 1985; Sun, 2002; Chen and Li, 2011). Thus, the deposits in these regions can provide essential information on their aridification. Recently, some long and continuous paleoclimatic records from drylands in northwest China have confirmed enhanced aridity in the mid-Pliocene. For example, *Ephedra and* Chenopodiaceae pollen characterize the Pliocene sporopollen assemblage of the Kuche Formation, north of the Tarim Basin (Cao et al., 2001), while, *Ephedra*, *Atremisia* and Chenopodiaceae dominate in the southern part of the Tarim Basin (Cao et al., 2001). In the Jiuxi Basin, dry herbs replaced temperate broadleaved trees at ~3.6 Ma (Fig. 3h) (Ma et al., 2005). Palynological assemblages for the Yahu section and F2 site in the central and northwest Qaidam Basin also suggest

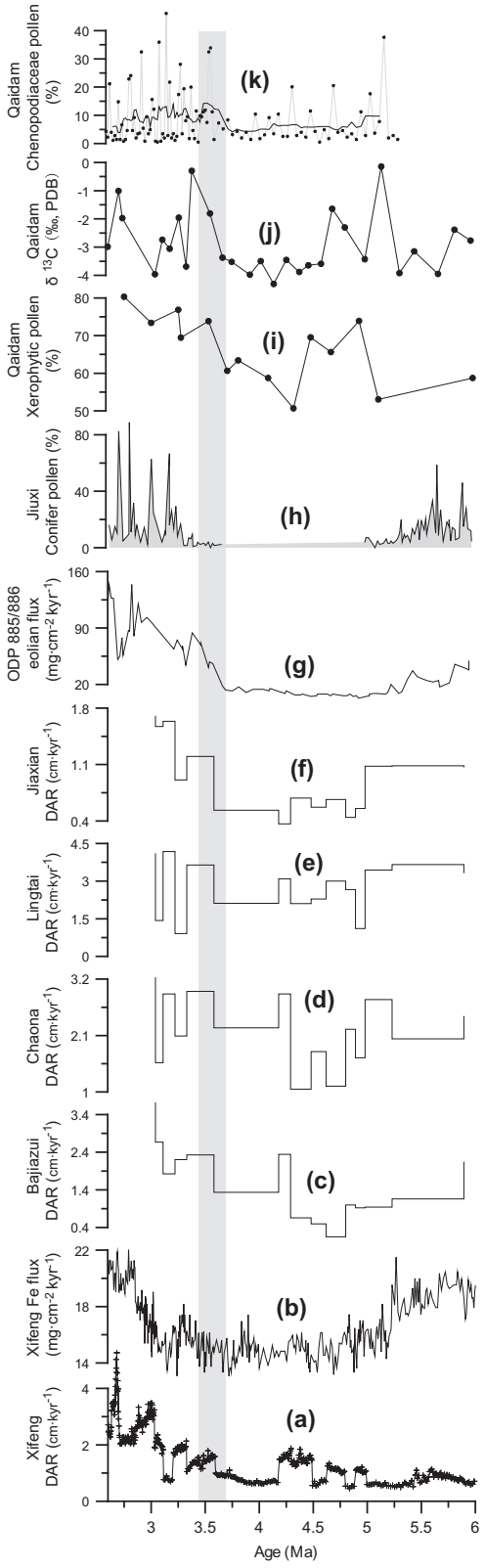

Fig. 3. Comparison of dust accumulation rates and Fe flux at Xifeng, dust accumulation rates at Bajiazui (An et al., 2001), Chaona (Song et al., 2000), Lingtai (Ding et al., 1998) and Jiaxian (Qiang et al., 2001), eolian flux at ODP 885/886 (Rea et al., 1998), Conifer pollen content at Jiuxi (Ma et al., 2005), and Xerophytic pollen content in the F2 site (Wang et al., 1999), Chenopodiaceae pollen content in the Yahu section (Wu et al., 2011) as well $\delta^{13}C$ in the HT section (Zhuang et al., 2011) in the Qaidam Basin.

that an environmental shift occurred at about 3.6 Ma leading to decreased percentages of thermophilous subtropical tree pollen and increased contributions from xerophytic plants, such as *Ephedra, Artemisia* and Chenopodiaceae, indicating a widely spreading steppe in response to cooler and drier climatic conditions (Fig. 3i, j) (Wang et al., 1999; Wu et al., 2011). The positive shift in $\delta^{13}C$ in the HT section in the Qaidam Basin also points to this strengthened aridity event in the interior drylands (Fig. 3k) (Zhuang et al., 2011). It may be argued that the increase in the supply of silty-sized materials and the subsequent expansion of drylands induced by tectonic uplift of the surrounding mountains may have increased the DAR and Fe-flux over the CLP. Our results, in combination with the information derived from the pollen and carbon isotope data from these areas, can, however, provide much more convincing evidence for the extensive aridity of the interior drylands in central Asia around 3.6 Ma.

4.2. Intensification of the East Asian winter monsoon ~3.6 Ma ago

A large body of evidence reveals that the eolian deposits in northern China ware mainly transported by the northwesterly Asian winter monsoon (Liu, 1985; An et al., 1990; Liu and Ding, 1998; Guo et al., 2008). The grain size of the eolian deposits, particularly the median grain size ratio after removal of pedogenic effects, is generally accepted as a measure of the vigor of the winter monsoon that carries dust from the interior drylands of northwest and central China areas downwind (e.g. An et al., 1991a).

The changes in grain-size (Fig. 4a) around 3.6 Ma agree well with the SiO_2/Al_2O_3 ratio at Xifeng (Fig. 4b) (Guo et al., 2004), and are also temporally rather consistent with the distinct increasing in the >19 μm fractions at Bajiazui (Fig. 4c) (An et al., 2001) and the >20 μm fractions at Jiaxian (Fig. 4d) (Qiang et al., 2001) at ~3.6 Ma, indicating a widespread and significant intensification of the winter monsoon over the CLP during this period.

When the dust source areas became tectonically active, more coarse-grained materials may also have become available in these regions during this interval, but they cannot be entrained and transported to the faraway CLP without some increase in wind energy. Furthermore, the evidence from isotopic and elemental composition has demonstrated that no significant changes in dust provenance for the eolian dusts occurred during the late Neogene period (Sun, 2005; Wang et al., 2007; Sun and Zhu, 2010). The present evidence from eolian records in CLP thus tends to support the view that the dust grain-size changes during late Neogene were mainly caused by changes in wind strength.

The East Asian winter monsoon also exerts a strong influence on the South China Sea by lowering the sea surface temperature and raising the productivity by bringing nutrients to the surface (Zheng et al., 2004), thus the records in the South China Sea can also provide information on the evolution of the winter monsoon. Some recent studies show that *N. dutertrei*, one of the typical winter monsoon proxies (Fig. 4e) (Jian et al., 2001), started to increase at ~3.5 Ma, with a more rapid rise at ~2.5 Ma, indicating strengthened winter monsoon intensity. Meanwhile, proxy records of increased productivity also indicate the growing influence of the EAWM beginning about 3.5 Ma ago and becoming more prominent at about 2.5 Ma (Fig. 4f and g) (Wan et al., 2007; Zheng et al., 2004; Clemens et al., 2008). Moreover, increases in the terrigenous component and in the $\delta^{13}C$ of black carbon in ODP 1148 (Fig. 4h and i) (Wan et al., 2007; Jia et al., 2003) around 3.5 Ma were also interpreted as an effect of intensification of the EAWM.

4.3. The characteristics of the East Asian summer monsoon during the mid-Pliocene

In the CLP, soils are basically frozen from late autumn to early spring (Guo et al., 2000), thus chemical weathering of loess mainly

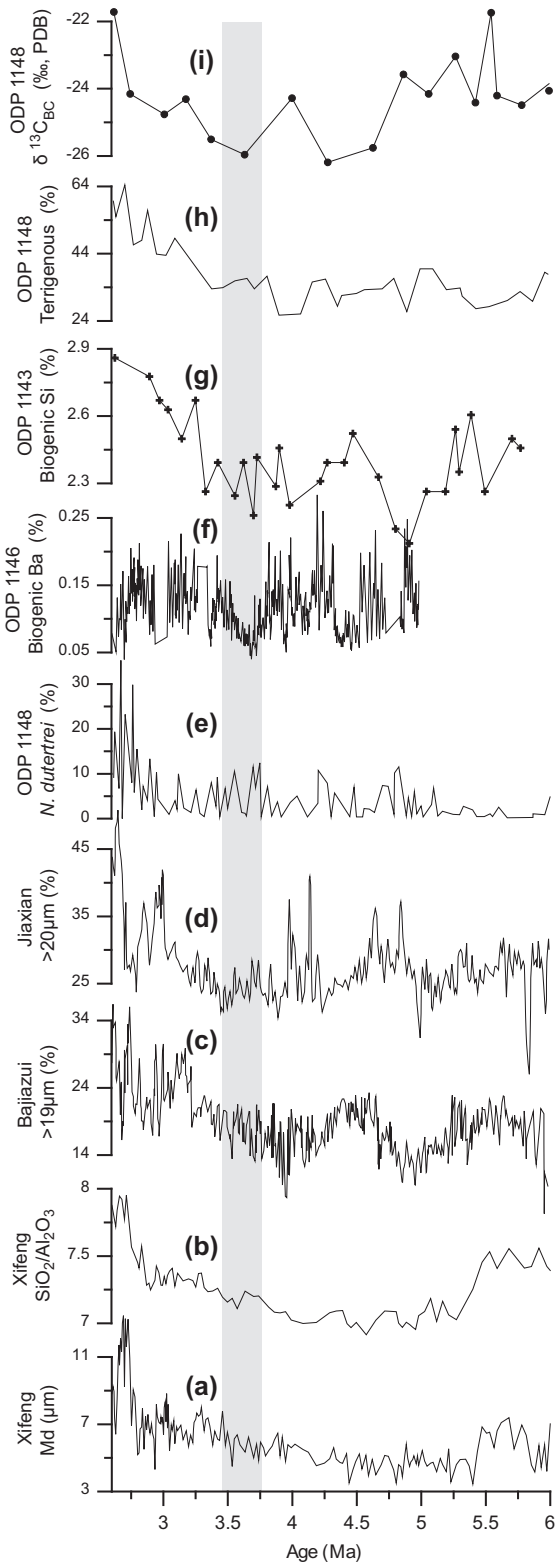

Fig. 4. Comparison of median grain size and SiO_2/Al_2O_3 (Guo et al., 2004) at Xifeng, >19 μm grain size at Bajiazui (An et al., 2001), >20 μm grain size at Jiaxian (Qiang et al., 2001), *N.dutertrei* (Zheng et al., 2004), the $\delta^{13}C$ of black carbon (Jia et al., 2003) and terrigenous (%) (Wan et al., 2007) at ODP 1148, biogenic Ba at ODP 1146 (Clemens et al., 2008) and biogenic Si at ODP 1143 (Wan et al., 2007).

depends upon summer temperatures and precipitation, which are closely linked to the strength of the summer monsoon. Generally, a strengthened southeast summer monsoon carries plentiful precipitation and results in the enhanced weathering intensity of soils in the CLP (Liu, 1985; Guo et al., 2000; Ge et al., 2006). Our results indicate that strong chemical weathering characterized the soils in the Xifeng Red Clay sequence (Fig. 5a and b) and the Xihe late Miocene–Pliocene loess-soil sequence (Fig. 2h and j) from 5.4 to 3.6 Ma, suggesting high summer temperature and precipitation owing to the effects of a strong summer monsoon. After ~3.6 Ma, chemical weathering intensity declined markedly and less mature soils in the Xifeng section (Fig. 5a and b), indicate a weakened summer monsoon.

The decrease in strength of the EASM after 3.6 Ma is also demonstrated by changes in the degree of pedogenesis in soils in the Xihe and Xifeng sections. Soils from the Xihe section, with an age of 6.0–4.1 Ma, generally have a strong argillic (Bt) horizon, with moderate to strong prismatic structure and mostly dark reddish-brown color. Micromorphological examination reveals that soils in the Xihe section are mostly characterized by a fragmented microstructure with strong decalcification and rubification of the groundmass. Abundant clay illuvial features, in the forms of clay coatings and intercalations, were observed in most of the soils, and strong rubification along with a few illuvial features were also recorded in some loess layers (Ge and Guo, 2010), indicating strong pedogenesic influence. In the upper 25 m of the Xifeng section (<3.6 Ma), the soils are characterized by light yellow–brown color and weak coarse subangular blocky structure. Most of them can be identified as Bw or weak Bt horizons. These results suggest that the degree of pedogenesis in soils postdating the mid-Pliocene became obviously weakened. This is also broadly consistent with previous pedostratigraphic studies on the Lingtai Red Clay sequence, which showed much more developed soils between 5.3 and 3.8 Ma than after 3.8 Ma (Ding et al., 1999).

By now, there is a growing body of evidence suggestive of, or consistent with, relatively warm and humid climates during the early Pliocene (~5.3–3.6 Ma) and cooler and drier climates after that time. The evidence mainly centers on interpretation of the weathering intensity of soils, mollusk faunas and vegetation composition in the CLP.

Using the difference between bulk samples which have been modified by post-depositional weathering processes and the quartz of eolian deposits almost free from weathering in the CLP deposits, Liu et al. (2007) defined a grain-size weathering index (Gw) ($Gw = (Md_Q - Md_B)/Md_Q \times 100\%$, where Md_Q and Md_B represent the mean grain-size of the quartz content of eolian deposits and of bulk samples, respectively) (Fig. 5c), and suggested that the eolian deposits at Xifeng experienced strong weathering for the Late Miocene to Middle Pliocene period, and weaker weathering during the Late Pliocene and Quaternary. For the Baishui Red Clay sequence, the declining CIA and LOI (Fig. 5d and e) from ~3.6 to 2.6 Ma also show a marked weakening of chemical weather intensity (Xiong et al., 2010). This also is rather consistent with the results from the Xifeng Red Clay sequence, suggesting that cool and dry climatic conditions became a dominant characteristic of the CLP environment after ~3.6 Ma. Moreover, the reduction in redness (a^*) (Fig. 5f) in the fluviolacstrine Sikouzi section from 3.6 to 2.6 Ma was also regard as a decrease in weathering influencing the oxidation of iron-bearing minerals owing to a more arid and cooler climate (Jiang et al., 2007), coinciding with the results derived from the eolian deposits.

Fossils mollusk faunas at Xifeng (Fig. 5g and h) (Wu et al., 2006) and Dongwan (Fig. 5i) (Li et al., 2008) in the eastern and western CLP have been studied. The records show a predominance of thermo-humidiphilous and meso-xerophilous mollusks between 5.4–3.5 Ma, and a near absence of cold-aridiphilous mollusks during this time. After that, the cold-aridiphilous species replaced the thermo-humidiphilous species becoming dominant in the mollusk fossil assemblages at Xifeng. This suggests relatively humid and

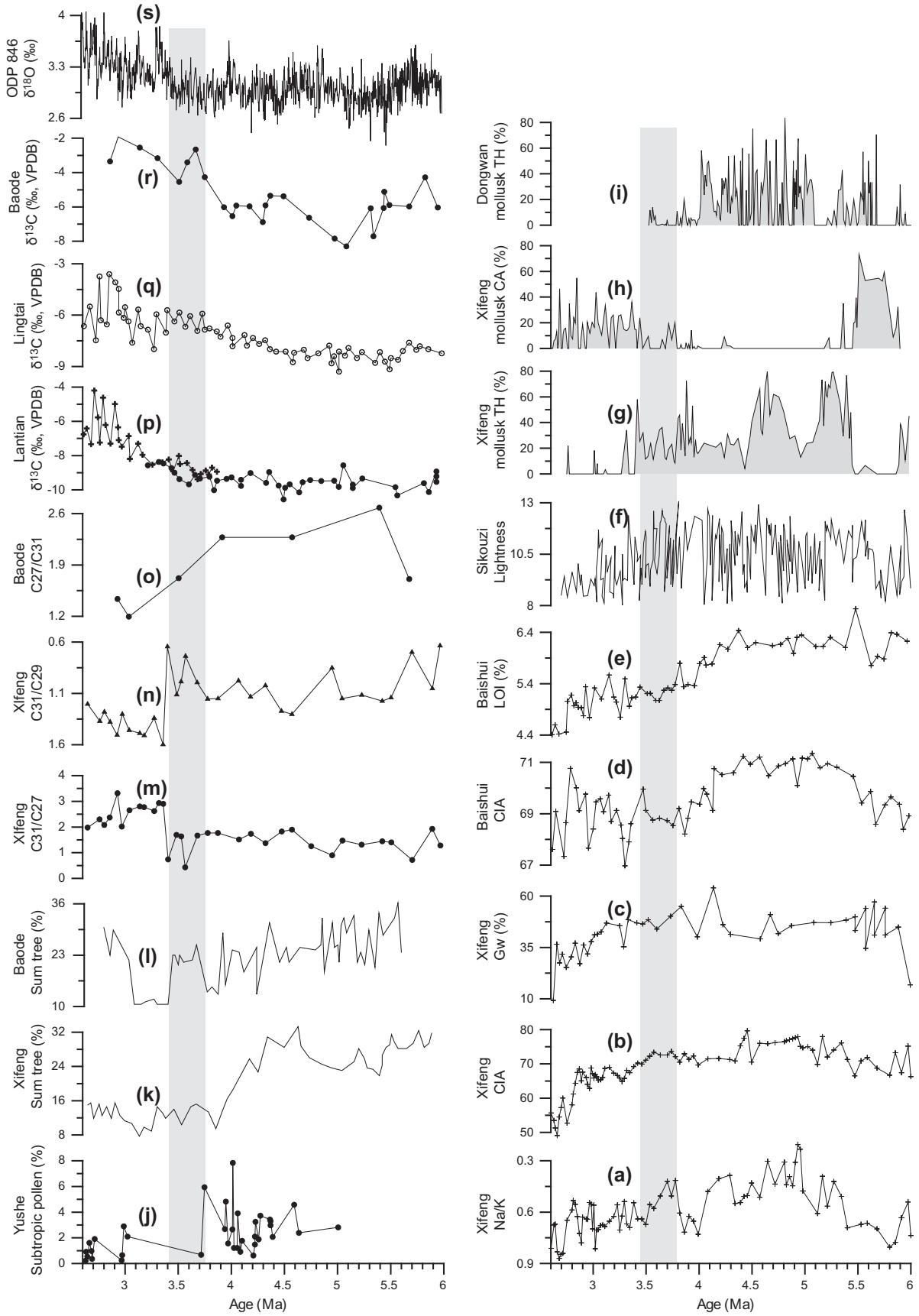

Fig. 5. Comparison of the Na/K ratio, $(CaO^* + Na_2O + MgO)/TiO_2$ ratio, Gw index (Liu et al., 2007) at Xifeng, CIA and LOI at Baishui (Xiong et al., 2010), redness (a^*) at Sikouzi (Jiang et al., 2007), mollusk fossils assemblages at Xifeng (Wu et al., 2006) and Dongwan (Li et al., 2008), subtropical pollen content at Yushe (Shi et al., 1993), tree pollen sum(Wang et al., 2006; Li et al., 2011) and the *n*-alkanes component of leaf waxes (C_{31}/C_{27}, $C_{31}/_{29}$) at Xifeng (Liu et al., 2008) and Baode (Bai et al., 2009), and the $\delta^{13}C$ of soil carbonate at Lantian (An et al., 2005; Kaakinen et al., 2006), Lingtai (Ding and Yang, 2000) and Baode (Suarez et al., 2011).

warm conditions in the CLP from 5.4 to 3.5 Ma, and more arid and cooler conditions after 3.5 Ma.

In the CLP, the variations in vegetation patterns may shed light on past climates. Many studies of Pliocene pollen assemblages (Wang et al., 2006; Li et al., 2011) and the *n*-alkane component of leaf waxes in paleosoil (Liu et al., 2008), as well as the soil carbonate $\delta^{13}C$ at different locations in the CLP (An et al., 2005), have all demonstrated that the vegetation in the CLP experienced a remarkable transition from forest or forest steppe to a steppe landscape in the mid-Pliocene, indicating that the climate of the CLP underwent a remarkable change from a warm and humid climate to dry and cool climatic conditions during this period. At Yushe, the palynological evidence shows that the mixed coniferous broadleaf forest along with subtropical taxa developed before ~3.6 Ma, while after this, grassland expanded rapidly (Fig. 5j) (Shi et al., 1993). Lingtai pollen data reveal high percentages of arboreal taxa and shrubs with subtropical *Carya* and *Tsuga* between 5.8 and 3.4 Ma (Wu, 2001). In both the Xifeng (Fig. 5k) (Wang et al., 2006) and northernmost Luzigou (Fig. 5l) (Li et al., 2011) Red Clay sections, the pollen assemblages also show a significant decrease in arboreal abundance and the disappearance of subtropical taxa, indicating a marked vegetation shift from temperate forest/forest steppe plants to typical grassland at ~3.6 Ma ago. The ratios of C_{31}/C_{27} and C_{31}/C_{29} at Xifeng (Fig. 5m and n) (Liu et al., 2008) and Baode (Fig. 5o) (Bai et al., 2009) both showed an increase at 3.5–3.8 Ma that indicates that the grasses replaced woody plants suddenly and dominated the CLP. Meanwhile, the $\delta^{13}C$ of soil carbonates at multiple Red Clay sections in the CLP, such as Lantian (Fig. 5p) (An et al., 2005; Kaakinen et al., 2006), Lingtai (Fig. 5q) (Ding and Yang, 2000) and Baode (Fig. 5r) (Suarez et al., 2011), all show a distinct rise at ~3.6 Ma. The increasing $\delta^{13}C$ values from ~3.6 to 2.6 Ma, were interpreted as reflecting a higher proportion of C_4 plants in response to the southward retreat of the summer monsoon front (Passey et al., 2009; Suarez et al., 2011).

Together these lines of evidence imply an inactive EASM after ~3.6 Ma, consistent with the results presented here. This runs contrary to the suggestion, based on the increase in MS in the Pliocene Red Clay (Sun et al., 1998; Clemens et al., 2008) that the summer monsoon became stronger after that time. Although MS is generally considered to be an indicator of monsoon strength in the younger loess-paleosol strata (An et al., 1991b), there is a significant discrepancy between the MS values and pedogenic development in the Red Clay. In most of the Red Clay sequences, the MS value is much lower overall than in the paleosols in the overlying loess, whereas pedogenic development in the Red Clay is apparently stronger than in the soils in the Quaternary loess (Ding et al., 1999). There are at least three possible explanations for this inconsistency: (1) the relationship of MS to climate is not straightforward (Heller and Evans, 1995; Maher and Thompson, 1995); (2) MS values may have been reduced under more humid conditions, probably due to frequent groundwater oscillations and poor drainage (Ding et al., 1999; Guo et al., 2001), and (3) more advanced weathering may have led to the progression from magnetite/maghemite with high MS values to haematite of much lower susceptibility provided the soils were sufficiently aerobic (Torrent et al., 2006; Hao et al., 2009). In addition, other factors such as the initial eolian inputs (Sun and Liu, 2000) and vegetation decay (Meng et al., 1997) have also been suggested as factors influencing the MS of eolian deposits. Thereafter, caution is needed when using MS for paleoclimate reconstruction, especially for the pre-Quaternary eolian deposits.

The contemporaneous Dongwan and Xihe loess-soil sequences recently found in the Western CLP (Hao and Guo, 2004) and the West Qinling (Ge and Guo, 2010) may provide some extra support for the possibility that the MS of the Red Clay in the eastern CLP may have been affected by post-depositional processes. Compared with the Red Clay in the eastern CLP, the MS values in the Xihe and Dongwan sequences are characterized by much higher values and larger fluctuations in amplitude between loess and soil layers (Fig. 6), associated with much clearer alternations of loess and soil layers than in most of the Red Clay sequences. This is consistent with the inference of syn- and post-depositional modification of the sedimentary characteristics and the MS values for most of the Red Clay sequences in the eastern CLP (Ding et al., 1999; Guo et al., 2001). Furthermore, the long-term increasing trend of MS is absent in the Xihe and Dongwan sections (Fig. 6) suggesting that the rise of MS of the Pliocene Red Clay may be attributed to the gradual diminution of post-depositional influences.

4.4. Possible links of the East Asian climate changes with the uplift of Tibetan Plateau and global cooling in mid-Pliocene

Two main factors have been invoked to explain the changes of the Asian monsoon circulation and the aridity in the interior of Asia in the mid-Pliocene. One is TP uplift, which may have played an important role in aridification through modulating the atmospheric circulation and its barrier effect to moisture (e.g., An et al., 2001), as earlier climate simulations suggested. The other is ongoing global cooling and the expansion of the Arctic ice-sheet, which is likely to have had a major impact on the intensity of the winter Siberian High, resulting in higher continental aridity in central Asia and a stronger EAWM (e.g., Guo et al., 2004; Lu et al., 2010).

During the mid-Pliocene period (~3.6 Ma), several observations point to changes in the tectonic evolution of the TP and its surroundings and these are interpreted as responses to the uplift of the plateau (Li et al., 1997). For example, in some basins along the northeastern and eastern margins of TP, widely distributed conglomerates replaced lacustrine/fluvial deposits at ~3.6 Ma ago (e.g., Li et al., 1997; Metivier et al., 1998; Zheng et al., 2000; Fang et al., 2005), and the sediment flux filling these basins increased significantly at the same time, coinciding with the onset of rapid exhumation in some parts of the TP, such as the West Kunlun Mountain (Wang et al., 2003), southern Tibet (Wang et al., 2008) and eastern Tibet (Xiang et al., 2007). Meanwhile, some faults, for example the Altyn and Lajishan faults, experienced significant strike slipping in the mid-Pliocene, leading to a widespread depositional hiatus on the margins of the Qaidam, Guide and Linxia basins around ~3.6 Ma (Yuan, 2003; Hough et al., 2011). Moreover, in the Siwalik and the Bay of Bengal, the deposition rates (Tauxe and Opdyke, 1982; Burbank, 1992) and the terrigenous flux from the TP (Yokoyama et al., 1990) show rapid increases around 3.5 Ma ago. On the basis of these observations, intense uplift of the TP around 3.6 Ma was proposed by some authors. Some authors have suggested that after 3–4 Ma, parts if not the whole of Tibet, could have risen from a low plateau below ~2000 m high to its present height (Li and Fang, 1999; Li et al., 1997; Pares et al., 2003).

As earlier simulations mostly demonstrated, the growing elevation and expansion of the TP would significantly alter the thermally forced circulation, intensify central Asian aridity and enhance both continental-scale summer and winter monsoon circulations in Asia (e.g., Kutzbach et al., 1989; Broccoli and Manabe, 1992; An et al., 2001; Liu and Yin, 2002; Zhang et al., 2007). This implies that uplift and expansion of the TP around 3.6 Ma would not only have increased the aridity of interior drylands in central Asia but would also have strengthened both the summer and winter monsoons in East Asia.

However, all the evidence in this study shows that although aridity and the ESWM strengthened after ~3.6 Ma, the EASM weakened from the mid-Pliocene to the present day. The model simulations indicate that this pattern of changes in the strength of the East Asian monsoon and central Asian aridification is

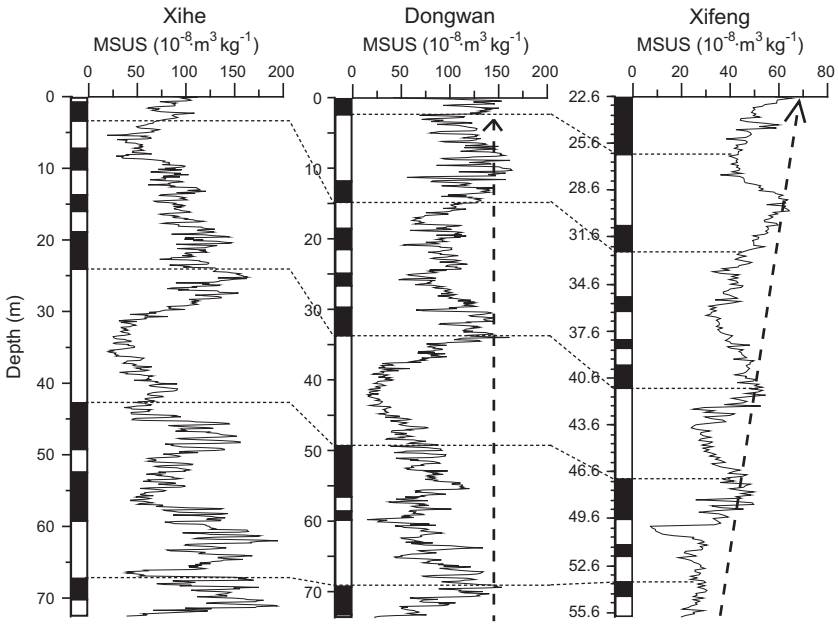

Fig. 6. Comparison of the magnetostratigraphy and magnetic susceptibility records of Xifeng Red Clay, Dongwan and Xihe Pliocene loess-soil sequences. Black/white bars in this figure indicate normal/reverse polarity.

difficult to explain by TP uplift. Therefore our evidence does not support the view that uplift of the Tibetan Plateau led to the dramatic changes in East Asian climate from the mid-Pliocene onwards. Although the evidence for tectonic activity in the TP and its surroundings seems robust, the range and the height of the uplift remain uncertain. Moreover, some recent studies have also proposed that the increases in sedimentation rate and grain size in deposits from the mid-late Pliocene (2–4 Ma) period, from which inferences regarding TP uplift have been derived, may instead be a response to synchronous global climate changes in the mid- to late Pliocene (Zhang et al., 2001; Molnar, 2004).

These considerations point to the alternative explanation for the mid-Pliocene changes in the East Asian monsoon and the aridification of the continental interior, namely ongoing global cooling (Ding et al., 1995; Guo et al., 2004; Lu et al., 2010). All the data in this study show that the changes in the strength of East Asian monsoon and aridifictaion in central Asia between 6.0 and 2.6 Ma, indicated by the grain-size, sedimentation rate, Fe-flux, fossils mollusk assemblages and pollen indices of the eolian deposits in the CLP, all show consistent changes with the ODP 846 $\delta^{18}O$ record (Fig. 5s) (Shackleton et al., 1995), an indication of global ice-volume, implying that the ongoing global cooling may have played an important role in controlling the East Asian climate changes. This idea is also supported by new mid-Pliocene simulations (Zhang et al., 2012) with the low-resolution version of the Norwegian Earth System Model (NorESM-L), within the PlioMIP framework (Haywood et al., 2011). In this simulation, the pre-industrial control experiment designed to test its ability to simulate modern climate realistically uses the land-sea mask, topography and the ice sheets and vegetation data for year 1850 and the orbital parameter values for 1950 (Berger, 1978). All the geographic boundary and aerosol conditions are taken from the CESM (Vertenstein et al., 2010), and the modern bathymetry is initialized from the temperature and salinity values used by Levitus and Boyer (1994). Meanwhile, the atmospheric greenhouse gases and solar constant are set to 280 ppm and 1370 W m^{-2}, respectively. With these boundary conditions, the pre-industrial control experiment is run for 1500 yr. Compared to the pre-industrial simulation, the major changes in the mid-Pliocene boundary conditions include the increased atmosphere CO_2 level, from 280 ppmv to 405 ppmv, reduced land ice in Greenland and Antarctica, and a much more complete vegetation cover, while topography does not change significantly. Comparison of the simulation with observations demonstrates that NorESM-L simulates a realistic pre-industrial climate. The simulated mid-Pliocene precipitation is higher than the pre-industrial (Fig. 7). The simulation indicates that the summer (winter) monsoon is weakened (intensified) (Fig. 7a and b), and aridity

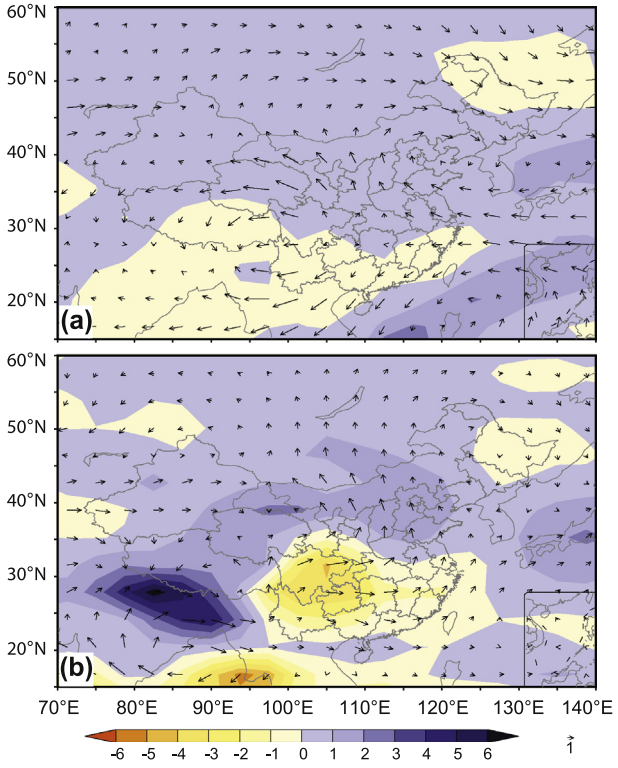

Fig. 7. NorESM-L simulated anomalies of near surface winds (arrows, m/s) and precipitation (shaded, mm/d) between the mid-Pliocene and the pre-industrial, (a) for winter DJF and (b) for summer JJA.

in central Asia is strengthened from the mid-Pliocene, agreeing well with our geological results. Thus, the new simulation supports the idea that ongoing cooling is the main reason for the weakened summer monsoon and the intensified winter monsoon from the mid-Pliocene to the present day. However, even though our results indicate that the ongoing high-latitude cooling and the consequent expansion of the Northern Hemisphere ice-sheets played a major role in the evolution of the East Asian monsoon and the aridification in central Asia from the mid-Pliocene, we do not exclude the possible influence of TP uplift on the East Asian environmental changes since ~3.6 Ma. We can, however, conclude that the contribution from TP uplift to the monsoon changes in East Asia from the mid-Pliocene onwards is much less important than the contribution from the ongoing cooling.

5. Conclusion

In this paper, several climate proxies, i.e., particle size, dust accumulation rates, depositional flux and chemical weathering intensity of the Xifeng Red Clay sequence in the eastern CLP and the contemporaneous Xihe Pliocene eolian deposits in West Qinling were analyzed. Combining these data from the Xifeng and Xihe sections, the multi-proxy records from the northwestern arid areas in China and the deposits from the South China Sea, we reconstruct the changing strength of winter and summer monsoons in East Asia as well as the aridification history of the drylands in central Asia between 6.0 Ma and 2.6 Ma. The results show that the aridification and the ESWM both strengthened after ~3.6 Ma, whereas, by contrast, the EASM weakened. These reconstructions from the geological data are in disagreement with previous numerical simulations of the climatic effects of TP uplift. These predicted simultaneous intensification of both summer and winter monsoons as well strengthened aridity in central Asia. Thus, we propose that ongoing global cooling and the expansion of the Arctic ice-sheet rather than Tibetan uplift have played a dominant role in the enhanced aridification and winter monsoon strength, alongside a weakened summer monsoon in East Asia since the mid-Pliocene. This conclusion is also supported by recent modeling results.

Acknowledgements

Thanks are extended to Drs. Chunxia Zhang, Qingzhen Hao and Haibin Wu from the institute of Geology and Geophysics, China Academy of Sciences for constructive comments and helpful discussion. This work was supported by the National Nature Science Foundation of China (41002125) and the National Basic Research Program of China (2010CB950200).

References

Abe, M., Kitoh, A., Yasunari, T., 2003. An evolution of the Asian summer monsoon associated with mountain uplift-simulation with the MRI atmosphere–ocean coupled GCM. Journal of the Meteorological Society of Japan 81, 909–933.

An, Z.S., Liu, T.S., Lu, Y.C., Porter, S.C., Kukla, G., Wu, X.H., Hua, Y.M., 1990. The long-term paleomonsoon variation recorded by the loess-paleosol sequence in Central China. Quaternary International 7–8, 91–95.

An, Z.S., Kukla, G., Porter, S.C., Xiao, J.L., 1991a. Late Quaternary dust flow on the Chinese Loess Plateau. Catena 18, 125–132.

An, Z.S., Kukla, G., Porter, S.C., Xiao, J.L., 1991b. Magnetic susceptibility evidence of monsoon variation on the Loess Plateau of central China during the last 130,000 years. Quaternary Research 36, 29–36.

An, Z.S., Kutzbach, J.E., Prell, W.L., Porter, S.C., 2001. Evolution of Asian monsoons and phased uplift of the Himalaya–Tibetan plateau since Late Miocene times. Nature 411, 62–66.

An, Z.S., Huang, Y.S., Liu, W.G., Guo, Z.T., Steven, C., Li, L., Warren, P., Ning, Y.F., Cai, Y.J., Zhou, W.J., Lin, B.H., Zhang, Q.L., Cao, Y.N., Qiang, X.K., Chang, H., Wu, Z.K., 2005. Multiple expansions of C_4 plant biomass in East Asia since 7 Ma coupled with strengthened monsoon circulation. Geology 33, 705–708.

Bai, Y., Fang, X.M., Nie, J.S., Wang, Y.L., Wu, F.L., 2009. A preliminary reconstruction of the paleoecological and paleoclimatic history of the Chinese Loess Plateau from the application of biomarkers. Palaeogeography, Palaeoclimatology, Palaeoecology 271, 161–169.

Berger, A.L., 1978. Long-term variations of daily insolation and Quaternary climatic changes. Journal of Atmospheric Sciences 35, 2362–2367.

Broccoli, A., Manabe, S., 1992. The effects of orography on midlatitude Northern Hemisphere dry climates. Journal of Climate 5, 1181–1201.

Buggle, B., Glaser, B., Hambach, U., Gerasimenko, N., Markovic, S., 2011. An evaluation of geochemical weathering indices in loess-paleosol studies. Quaternary International 240, 12–21.

Burbank, D.W., 1992. Causes of recent Himalayan uplift deduced from deposited patterns in the Ganges basin. Nature 357, 680–683.

Cao, M.Z., Chen, J.H., Wu, B., 2001. The nonmarine Lower and Upper Tertiary in Tarim Basin. In: Zhou, Z.Y. (Ed.), Stratigraphy of the Tarim Basin. Science Press, Beijing, pp. 280–324.

Chen, J., Li, G.J., 2011. Geochemical studies on the source region of Asian dust. Science in China Series D: Earth Sciences 54, 1279–1301.

Chen, J., An, Z.S., Liu, L.W., Ji, J.F., Yang, J.D., Chen, Y., 2001. Variations in chemical compositions of the eolian dust in Chinese Loess Plateau over the past 2.5 Ma and chemical weathering in the Asian inland. Science in China Series D: Earth Sciences 44, 403–413.

Clemens, S.C., Prell, W.L., Sun, Y.B., Liu, Z.Y., Chen, G.S., 2008. Southern hemisphere forcing of Pliocene δ18O and the evolution of Indo-Asian monsoons. Paleoceanography 23, PA4210. doi:4210.1029/2008PA001638.

Ding, Z.L., Yang, S.L., 2000. C3/C4 vegetation evolution over the last 7.0 Myr in the Chinese Loess Plateau: evidence from pedogenic carbonate $\delta^{13}C$. Palaeogeography, Palaeoclimatology, Palaeoecology 160, 291–299.

Ding, Z.L., Liu, T.S., Rutter, N.W., Yu, Z.W., Guo, Z.T., Zhu, R.X., 1995. Ice-volume forcing of East Asian winter monsoon variations in the past 800,000 years. Quaternary Research 44, 149–159.

Ding, Z.L., Sun, J.M., Liu, T.S., Zhu, R.X., Yang, S.L., Guo, B., 1998. Wind-blown origin of the Pliocene red clay formation in the central Loess Plateau, China. Earth and Planetary Science Letters 161, 135–143.

Ding, Z.L., Xiong, S.F., Sun, J.M., Yang, S.L., Gu, Z.Y., Liu, T.S., 1999. Pedostratigraphy and paleomagnetism of a ~7.0 Ma eolian loess-red clay sequence at Lingtai, Loess Plateau, north-central China and the implications for paleomonsoon evolution. Palaeogeography, Palaeoclimatology, Palaeoecology 152, 49–66.

Fang, X.M., Yan, M.D., Voo, R.V.D., Rea, D.K., Song, C.H., Parés, J.M., Gao, J.P., Nie, J.S., Dai, S., 2005. Late Cenozoic deformation and uplift of the NE Tibetan Plateau: Evidence from high-resolution magnetostratigraphy of the Guide Basin, Qinghai Province, China. Geological Society of America Bulletin 117, 1208–1225.

Ge, J.Y., Guo, Z.T., 2010. Neogene eolian deposits within the West Qinling Mountains: climate and tectonic implications. Chinese Science Bulletin 55, 1483–1487.

Ge, J.Y., Guo, Z.T., Hao, Q.Z., 2006. Spatial variations of weathering intensity in the Loess Plateau at characteristic timeslices and the climate gradients. Quaternary Science 26, 962–968.

Ge, J.Y., Guo, Z.T., Zhan, T., Yao, Z.Q., Deng, C.L., Oldfield, F., 2012. Magnetostratigraphy of the Xihe loess-soil sequence and implication for late Neogene deformation of the West Qinling Mountains. Geophysical Journal International 189, 1399–1408.

Guo, Z.T., 2003. Uplifting of Tibetan Plateau and the eolian deposits in China. In: Zheng, D. (Ed.), The Formation and the Environmental Development on the Tibetan Plateau. Hebei Science Press, Hebei, pp. 70–79.

Guo, Z.T., Biscaye, P., Wei, L.Y., Chen, X.H., Peng, S.Z., Liu, T.S., 2000. Summer monsoon variations over the last 1.2 Ma from the weathering of loess-soil sequences in China. Geophysical Research Letters 27, 1751–1754.

Guo, Z.T., Peng, S.Z., Hao, Q.Z., Biscaye, P.E., Liu, T.S., 2001. Origin of the Miocene–Pliocene Red-Earth Formation at Xifeng in Northern China and implications for paleoenvironments. Palaeogeography, Palaeoclimatology, Palaeoecology 170, 11–26.

Guo, Z.T., Ruddiman, W.F., Hao, Q.Z., Wu, H.B., Qiao, Y.S., Zhu, R.X., Peng, S.Z., Wei, J.J., Yuan, B.Y., Liu, T.S., 2002. Onset of Asian desertification by 22 Myr ago inferred from loess deposits in China. Nature 416, 159–163.

Guo, Z.T., Peng, S.Z., Hao, Q.Z., Biscaye, P.E., An, Z.S., Liu, T.S., 2004. Late Miocene–Pliocene development of Asian aridification as recorded in the Red-Earth Formation in northern China. Global and Planetary Change 41, 135–145.

Guo, Z.T., Sun, B., Zhang, Z.S., Peng, S.Z., Xiao, G.Q., Ge, J.Y., Hao, Q.Z., Qiao, Y.S., Liang, M.Y., Liu, J.F., 2008. A major reorganization of Asian climate by the early Miocene. Climate of the Past 4, 153–174.

Guo, Z.T., Ge, J.Y., Xiao, G.Q., Hao, Q.Z., Wu, H.B., Zhan, T., Liu, L., Qin, L., Zeng, F.M., Yuan, B.Y., 2010. Comment on "Mudflat/distal fan and shallow lake sedimentation (upper Vallesian–Turolian) in the Tianshui Basin, Central China: Evidence against the late Miocene eolian loess" by A.M. Alonso-Zarza, Z. Zhao, C.H. Song, J.J. Li, J. Zhang, A. Martín-Pérez, R. Martín-García, X.X. Wang, Y. Zhang and M.H. Zhang [Sedimentary Geology 222 (2009) 42–51]. Sedimentary Geology 230, 86–89.

Hao, Q.Z., Guo, Z.T., 2004. Magnetostratigraphy of a late Miocene–Pliocene loess-soil sequence in the western Loess Plateau in China. Geophysical Research Letters 31, L09209. doi:09210.01029/02003GL019392.

Hao, Q.Z., Guo, Z.T., 2007. Magnetostratigraphy of an early-middle Miocene loess-soil sequence in the western Loess Plateau of China. Geophysical Research Letters 34, L18305. doi:18310.11029/12007GL031162.

Hao, Q.Z., Oldfield, F., Bloemendal, J., Torrent, J., Guo, Z.T., 2009. The record of changing hematite and goethite accumulation over the past 22 Myr on the Chinese Loess Plateau from magnetic measurements and diffuse reflectance

spectroscopy. Journal of Geophysical Research 114, B12101. doi:12110.11029/12009JB00660.
Haywood, A.M., Dowsett, H.J., Robinson, M.M., Stoll, D.K., Dolan, A.M., Lunt, D.J., Otto-Bliesner, B., Chandler, M.A., 2011. Pliocene Model Intercomparison Project (PlioMIP): experimental design and boundary conditions (Experiment 2). Geoscientific Model Development 4, 445–456.
Heermance, R.V., Chen, J., Burbank, D.W., Wang, C., 2007. Chronology and tectonic controls of Late Tertiary deposition in the southwestern Tian Shan foreland, NW China. Basin Research 19, 599–632.
Heller, F., Evans, M.E., 1995. Loess Magnetism. Reviews of Geophysics 33, 211–240.
Hough, B.G., Garzione, C.N., Wang, Z.C., Lease, R.O., Burbank, D.W., Yuan, D.Y., 2011. Stable isotope evidence for topographic growth and basin segmentation: implications for the evolution of the NE Tibetan Plateau. Bulletin of the Geological Society of America 123, 168–185.
Hovan, S.A., Rea, D.K., Pisias, N.G., Shackleton, N.J., 1989. A direct link between the China loess and marine ^{18}O records: aeolian flux to the north Pacific. Nature 340, 296–298.
Jia, G.D., Peng, P.A., Zhao, Q.H., Jian, Z.M., 2003. Changes in terrestrial ecosystem since 30 Ma in East Asia: Stable isotope evidence from black carbon in the South China Sea. Geology 31, 1093–1096.
Jian, Z.M., Huang, B.Q., Kuhnt, W., Lin, H.L., 2001. Late Quaternary upwelling intensity and East Asian monsoon forcing in the South China Sea. Quaternary Research 55, 363–370.
Jiang, H.C., Ding, Z.L., Xiong, S.F., 2007. Magnetostratigraphy of the Neogene Sikouzi section at Guyuan, Ningxia, China. Palaeogeography, Palaeoclimatology, Palaeoecology 243, 223–234.
Jiang, H.C., Ji, J.L., Gao, L., Tang, Z.H., Ding, Z.L., 2008. Cooling-driven climate change at 12–11 Ma: multiproxy records from a long fluviolacustrine sequence at Guyuan, Ningxia, China. Palaeogeography, Palaeoclimatology, Palaeoecology 265, 148–158.
Kaakinen, A., Sonninen, E., Lunkka, J.P., 2006. Stable isotope record in paleosol carbonates from the Chinese Loess Plateau: implications for late Neogene paleoclimate and paleovegetation. Palaeogeography, Palaeoclimatology, Palaeoecology 237, 359–369.
Kukla, G.J., An, Z.S., 1989. Loess stratigraphy in Central China. Palaeogeography, Palaeoclimatology, Palaeoecology 72, 203–225.
Kukla, G., Heller, F., Liu, X.M., Xu, T.C., Liu, T.S., An, Z.S., 1988. Pleistocene climates in China dated by magnetic susceptibility. Geology 16, 811–814.
Kutzbach, J.E., Guetter, P.J., Ruddiaman, W.F., Prell, W.L., 1989. Sensitvity of climate to Late Cenozoic uplift in Southern Asia and the American West: numerical experiments. Journal of Geophysical Research 94, 18393–18407.
Levitus, S., Boyer, T., 1994. World Ocean Atlas Volume 4: Temperature, NOAA Atlas NESDIS 4. US Government Printing Office, Washington, DC, p. 117.
Li, J.J., Fang, X.M., 1999. Uplift of the Tibetan Plateau and environmental changes. Chinese Science Bulletin 44, 2117–2124.
Li, J.J., Fang, X.M., Van der Voo, R., Zhu, J.J., Mac Niocaill, C., Cao, J.X., Zhong, W., Chen, H.L., Wang, J., Wang, J.M., 1997. Late Cenozoic magnetostratigraphy (11–0 Ma) of the Dongshanding and Wangjiashan sections in the Longzhong Basin, western China. Geologie en Mijnbouw 76, 121–134.
Li, F.J., Rousseau, D.-D., Wu, N.Q., Hao, Q.Z., Pei, Y.P., 2008. Late Neogene evolution of the East Asian monsoon revealed by terrestrial mollusk record in Western Chinese Loess Plateau: From winter to summer dominated sub-regime. Earth and Planetary Science Letters 274, 439–447.
Li, X.R., Fang, X.M., Wu, F.L., Miao, Y.F., 2011. Pollen evidence from Baode of the northern Loess Plateau of China and strong East Asian summer monsoons during the Early Pliocene. Chinese Science Bulletin 56, 64–69.
Liu, T.S., 1985. Loess and the Environment. China Ocean Press, Beijing, 251pp.
Liu, T.S., Ding, Z.L., 1998. Chinese loess and the paleomonsoon. Annual Review of Earth and Planetary Sciences 26, 111–145.
Liu, X.D., Yin, Z.Y., 2002. Sensitivity of East Asian monsoon climate to the uplift of the Tibetan Plateau. Palaeogeography, Palaeoclimatology, Palaeoecology 183, 223–245.
Liu, J.F., Guo, Z.T., Hao, Q.Z., Peng, S.Z., Qiao, Y.S., Sun, B., Ge, J.Y., 2005. Magnetostratigraphy of the Miziwan Miocene eolian deposits in Qin'an County (Gansu Province). Quaternary Science 25, 503–508 (in Chinese with English abstract).
Liu, J.F., Qiao, Y.S., Guo, Z.T., 2007. The differences of grain size of quartz and bulk samples as an indicator of weathering intensity in the aeolian deposits. Quaternary Science 27, 270–276.
Liu, W.G., Zhang, P., Bin, S.Y., Huang, Y.S., Guo, Z.T., An, Z.S., 2008. Molecule fossil evidence for paleo-vegetation changes in the central of Chinese Loess Plateau during 7–2 Ma—Zhaojiachuan profile as an example. Quaternary Science 28, 806–811.
Lu, H., Wang, X., Li, L., 2010. Aeolian sediment evidence that global cooling has driven late Cenozoic stepwise aridification in central Asia. Geological Society, London, Special Publications 342, 29–44.
Ma, Y.Z., Fang, X.M., Li, J.J., Wu, F.L., Zhang, J., 2005. The vegetation and climate change during Neocene and Early Quaternary in Jiuxi Basin, China. Science in China Series D: Earth Sciences 48, 676–688.
Maher, B.A., Thompson, R., 1995. Paleorainfall reconstructions from pedogenic magnetic susceptibility variations in the Chinese loess and paleosols. Quaternary Research 44, 383–391.
Marković, S.B., Bokhorst, M.P., Vandenberghe, J., McCoy, W.D., Oches, E.A., Hambach, U., Gaudenyi, T., Jovanović, M., Zöller, L., Stevens, T., 2008. Late Pleistocene loess-palaeosol sequences in the Vojvodina region, north Serbia. Journal of Quaternary Science 23, 73–84.
Marković, S.B., Hambach, U., Catto, N., Jovanovic, M., Buggle, B., Machalett, B., Zöller, L., Glaser, B., Frechen, M., 2009. Middle and late Pleistocene loess sequences at Batajnica, Vojvodina, Serbia. Quaternary International 198, 255–266.
Marković, S.B., Hambach, U., Stevens, T., Kukla, G.J., Heller, F., McCoy, W.D., Oches, E.A., Buggle, B., Zöller, L., 2011. The last million years recorded at the Stari Slankamen (Northern Serbia) loess-palaeosol sequence. revised chronostratigraphy and long-term environmental trends. Quaternary Science Reviews 30, 1142–1154.
Meng, X.M., Derbyshire, E., Kemp, R.A., 1997. Origin of the magnetic susceptibility signal in Chinese loess. Quaternary Science Reviews 16, 833–839.
Metivier, F., Gaudemer, Y., Tapponnier, P., Meyer, B., 1998. Northeastward growth of the tibet plateau deduced from balanced reconstruction of two depositional areas: The Qaidam and Hexi Corridor basins, China. Tectonics 17, 823–842.
Molnar, P., 2004. Late Cenozoic increase in accumulation rates of terrestrial sediment: how might climate change have affected erosion rates? Annual Review of Earth Planetanry Science 32, 67–89.
Nesbitt, H.W., Markovics, G., Price, R.C., 1980. Chemical processes affecting alkalis and alkaline earths during continental weathering. Geochimica et Cosmochimica Acta 44, 1659–1666.
Pares, J.M., Van der Voo, R., Downs, W.R., Yan, M.D., Fang, X.M., 2003. Northeastward growth and uplift of the Tibetan Plateau: Magnetostratigraphic insights from the Guide Basin. Journal of Geophysical Research 108, 2017. doi:2010.1029/2001JB001349.
Passey, B.H., Ayliffe, L.K., Kaakinen, A., Zhang, Z., Eronen, J.T., Zhu, Y., Zhou, L., Cerling, T.E., Fortelius, M., 2009. Strengthened East Asian summer monsoons during a period of high-latitude warmth? Isotopic evidence from Mio-Pliocene fossil mammals and soil carbonates from northern China. Earth and Planetary Science Letters 277, 443–452.
Qiang, X.K., Li, Z.X., Powell, C., Zheng, H.B., 2001. Magnetiostratigraphic record of the late Miocene onset of the East Asian monsoon, and Pliocene uplift of northern Tibet. Earth and Planetary Science Letters 187, 83–93.
Qiao, Y.S., Guo, Z.T., Hao, Q.Z., Yin, Q.Z., Yuan, B.Y., Liu, T.S., 2006. Grain-size features of a Miocene loess-soil sequence at Qinan: implications on its origin. Science in China Series D: Earth Sciences 49, 731–738.
Rea, D.K., Snoeckx, H., Joseph, L.H., 1998. Late Cenozoic eolian deposition in the North Pacific: Asian drying, Tibetan uplift, and cooling of the northern hemisphere. Paleoceanography 13, 215–224.
Shackleton, N.J., Hall, M.A., Pate, D., 1995. Pliocene stable isotope stratigraphy of site 846. Proceedings of Ocean Drilling Programs, Scientific Results 138, 337–355.
Shi, N., Xin, C.J., Königsson, L.K., 1993. Late Cenozoic vegetational history and the Pliocene–Pleistocene boundary in the Yushe basin, SE Shanxi, China. Grana 32, 260–271.
Song, Y.G., Fang, X.M., Li, J.J., An, Z.S., Yang, D., Lu, L.Q., 2000. Age of red clay at Chaona section near eastern Liupan Mountain and its tectonic significance. Quaternary Science 20, 457–463.
Suarez, M.B., Passey, B.H., Kaakinen, A., 2011. Paleosol carbonate multiple isotopologue signature of active East Asian summer monsoons during the late Miocene and Pliocene. Geology 39, 1151–1154.
Sun, J.M., 2002. Provenance of loess material and formation of loess deposits on the Chinese Loess Plateau. Earth and Planetary Science Letters 203, 845–859.
Sun, J.M., 2005. Nd and Sr isotopic variations in Chinese eolian deposits during the past 8 Ma: Implications for provenance change. Earth and Planetary Science Letters 240, 454–466.
Sun, J.M., Liu, T.S., 2000. Multiple origins and interpretations of the magnetic susceptibility signal in Chinese wind-blown sediments. Earth and Planetary Science Letters 180, 287–296.
Sun, J.M., Zhu, X.K., 2010. Temporal variations in Pb isotopes and trace element concentrations within Chinese eolian deposits during the past 8 Ma: Implications for provenance change. Earth and Planetary Science Letters 290, 438–447.
Sun, D.H., An, Z.S., Shaw, J., Bloemendal, J., Sun, Y.B., 1998. Magnetostratigraphy and palaeoclimatic significance of Late Tertiary aeolian sequences in the Chinese Loess Plateau. Geophysical Journal International 134, 207–212.
Tauxe, L., Opdyke, N.D., 1982. A time framework based on magnetostratigraphy for the Siwalik sediments of the Khaur area, northern Pakistan. Palaeogeography, Palaeoclimatology, Palaeoecology 37, 43–61.
Torrent, J., Barrón, V., Liu, Q.S., 2006. Magnetic enhancement is linked to and precedes hematite formation in aerobic soil. Geophysical Research Letters 33, L02401, doi:02410.01029/02005GL024818.
Vertenstein, M., Craig, T., Middleton, A., Feddema, D., Fischer, C., 2010. CESM1.0.3 User's Guide. <http://www.cesm.ucar.edu/models/cesm1.0/cesm/cesmdoc/book1.html>.
Wan, S.M., Li, A.C., Clift, P.D., Stuut, J.-B.W., 2007. Development of the East Asian monsoon: Mineralogical andsedimentologic records in the northern South China Sea since 20 Ma. Palaeogeography, Palaeoclimatology, Palaeoecology 254, 561–582.
Wang, J., Wang, Y.J., Liu, Z.C., Li, J.Q., Xi, P., 1999. Cenozoic environmental evolution of the Qaidam Basin and its implications for the uplift of the Tibetan Plateau and the drying of central Asia. Palaeogeography, Palaeoclimatology, Palaeoecology 152, 37–47.
Wang, E.C., Wan, J.L., Liu, J.Q., 2003. Late Cenozoic geological evolution of the foreland basin bordering the West Kunlun range in Pulu area: constraints on timing of uplift of northern margin of the Tibetan Plateau. Journal of Geophysical Research 108, 2401. http://dx.doi.org/10.1029/2002JB001877.
Wang, L., Lü, H.Y., Wu, N.Q., Li, J., Pei, Y.P., Tong, G.B., Peng, S.Z., 2006. Palynological evidence for Late Miocene–Pliocene vegetation evolution recorded in the red

clay sequence of the central Chinese Loess Plateau and implication for palaeoenvironmental change. Palaeogeography, Palaeoclimatology, Palaeoecology 241, 118–128.
Wang, Y.X., Yang, J.D., Chen, J., Zhang, K.J., Rao, W.B., 2007. The Sr and Nd isotopic variations of the Chinese Loess Plateau during the past 7 Ma: implications for the East Asian winter monsoon and source areas of loess. Palaeogeography, Palaeoclimatology, Palaeoecology 249, 351–361.
Wang, G.C., I., G.J., Liu, C., 2008. Cenozoic tectonic history in the Gyirong-Nyalam area, south Tibet: Evidence from fission-track thermochronology. In: Garver, J.I., Montario, M. (Eds), Proceedings from the 11th International Conference on Thermochronometry, Anchorage, Alaska.
Wang, G.C., Cao, K., Zhang, K.X., Wang, A., Liu, C., Meng, Y.N., Xu, Y.D., 2011. Spatio-temporal framework of tectonic uplift stages of the Tibetan Plateau in Cenozoic. Science in China Series D: Earth Sciences 54, 29–44.
Wu, Y.S., 2001. Palynoflora at Late Miocene—Early Pliocene from Leijiahe of Lingtai, Gansu Province, China. Acta Botanica Sinica 43, 750–756.
Wu, N.Q., Pei, Y.P., Lu, H.Y., Guo, Z.T., Li, F.J., Liu, T.S., 2006. Marked ecological shifts during 6.2–2.4 Ma revealed by a terrestrial molluscan record from the Chinese Red Clay Formation and implication for palaeoclimatic evolution. Palaeogeography, Palaeoclimatology, Palaeoecology 233, 287–299.
Wu, F.L., Fang, X.M., Herrmann, M., Mosbrugger, V., Miao, Y.F., 2011. Extended drought in the interior of Central Asia since the Pliocene reconstructed from sporopollen records. Global and Planetary Change 76, 16–21.
Xiang, H.F., Wan, J.L., Han, Z.J., Guo, S.M., Zhang, W.X., Chen, L.C., Dong, X.Q., 2007. Geological analysis and FT dating of the large-scale risht-lateral strike-slip movement of the Red River fault zone. Science in China Series D: Earth Sciences 50, 331–342.
Xiong, S.F., Ding, Z.L., Zhu, Y.J., Zhou, R., Lu, H.J., 2010. A ~6 Ma chemical weathering history, the grain size dependence of chemical weathering intensity, and its implications for provenance change of the Chinese loess–red clay deposit. Quaternary Science Reviews 29, 1911–1922.
Yang, S.L., Ding, F., Ding, Z.L., 2006. Pleistocene chemical weathering history of Asian arid and semi-arid regions recorded in loess deposits of China and Tajikistan. Geochimica et Cosmochimica Acta 70, 1695–1709.
Yokoyama, K., Amano, K., Taira, A., Saito, Y., 1990. Mineralogy of silts from the Bengal Fan. Proceedings of Ocean Drilling Programs, Scientific Results 116, 59–73.
Yuan, D.Y., 2003. Tectonic Deformation Features and Space-time Evolution in Northeastern Margin of the Qinghai–Tibetan Plateau Since the Late Cenozoic Time. Institute of Geology, China Seismological Bureau.
Zhan, T., Guo, Z.T., Wu, H.B., Ge, J.Y., Zhou, X., Wu, C.L., Zeng, F.M., 2010. Thick Miocene eolian deposits on the Huajialing Mountains: the geomorphic evolution of the western Loess Plateau. Science in China Series D: Earth Sciences 54, 241–248.
Zhang, P.Z., Peter, M., Downs, W.R., 2001. Increased sedimentation rates and grain sizes 2–4 Myr ago due to the influence of climate change on erosion rates. Nature 410, 891–897.
Zhang, Z.S., Wang, H.J., Guo, Z.T., Jiang, D.B., 2007. Impacts of tectonic changes on the reorganization of the Cenozoic paleoclimatic patterns in China. Earth and Planetary Science Letters 257, 622–634.
Zhang, Z.S., Nisancioglu, K., Bentsen, M., Tjiputra, J., Bethke, I., Yan, Q., Risebrobakken, B., Andersson, C., Jansen, E., 2012. Pre-industrial and mid-Pliocene simulations with NorESM-L. Geoscientific Model Development 5, 523–533.
Zheng, H.B., Powell, C.M., An, Z.S., Zhou, J., Dong, G.R., 2000. Pliocene uplift of the northern Tibetan Plateau. Geology 28, 715–718.
Zheng, H.B., Powell, C.M., Rea, D.K., Wang, J.L., Wang, P.X., 2004. Late Miocene and mid-Pliocene enhancement of the East Asian monsoon as viewed from the land and sea. Global and Planetary Change 41, 147–155.
Zhuang, G.S., Hourigan, J.K., Koch, P.L., Ritts, B.D., Kent-Corson, M.L., 2011. Isotopic constraints on intensified aridity in Central Asia around 12 Ma. Earth and Planetary Science Letters 312, 152–163.